Formation of Giant Quasibound Cold Diatoms by Strong Atom-Cavity Coupling

B. Deb and G. Kurizki
Department of Chemical Physics, Weizmann Institute of Science, 76100 Rehovot, Israel
(February 1, 2008)

We show that giant quasi-bound diatomic complexes, whose size is typically hundreds of nm, can be formed by intra-cavity cold diatom photoassociation or photodissociation in the strong atom-cavity coupling regime.

34.10.+x,42.50.Fx,33.80.-b,42.50.Ct

arXiv:quant-ph/9902066v2 21 Feb 1999

Cold atoms exchanging single photons with cavity fields have been predicted to give rise to a variety of fascinating motional effects, both in the "good-cavity" (strong-coupling) regime of Rabi oscillations [1] and in the "bad-cavity" regime of nearly exponential decay [2]. Here we pose a question that has not been considered thus far: what happens when two identical cold atoms exchange a photon in the strong-coupling ("good-cavity") regime during a collision or diatomic dissociation? We show here that this regime gives rise to a novel, hitherto unexplored, interplay of molecular dynamics and cavity QED effects. The resulting two-atom dynamics is drastically modified at interatomic separations typically exceeding by 2 orders of magnitude those of currently investigated cold-atom collisional resonances in magneto-optical traps [3]. The predicted modification is due to the possibility of *diatomic quasibinding* (scattering resonance) in a potential well formed by the competing effects of the resonant dipole-dipole (RDDI) interaction and strong atom-cavity coupling. These effects have previously been shown by our group to *suppress energy exchange* between static atoms in a high-Q cavity [4]. The regime considered here drastically differs from that of atoms coupled by the RDDI in a "bad cavity" [5] or from that of coherently driven atoms in a cavity [6]. The quasibinding scattering potential formed by the RDDI and strong atom-cavity coupling is shown to support many vibrational diatom states. These states can be revealed in high-Q cavities by unusual spectral structures in resonance fluorescence and Raman scattering from colliding or dissociating pairs, as well as by sharp variation of the scattering cross-section as a function of their center-of-mass kinetic energy.

The model which we consider is that of a pair of cold two-level atoms interacting with a single-mode cavity field. Cavity losses (damping) will be accounted for later on. In the center-of-mass (COM) frame, the radial part of the interaction Hamiltonian H can be split into two parts. The kinetic part is

$$H_k = -\frac{\hbar^2}{2\mu}\frac{d^2}{dR^2} - \frac{\hbar^2 l(l+1)}{2\mu R^2} \qquad (1)$$

where $\mu = \frac{m_A m_B}{m_A+m_B}$ is the reduced mass, $R = \mid \vec{R}_A - \vec{R}_B \mid$ is the separation between atoms A and B and l represents the angular momentum quantum number. The other part is the adiabatic Hamiltonian [4]

$$\begin{aligned} H_{ad} &= H - H_k \\ &= \hbar\omega_A\sigma_z^{(A)} + \hbar\omega_B\sigma_z^{(B)} + \hbar\omega_c a^\dagger a \\ &+ \hbar(\kappa_A a\sigma_+^{(A)} + \kappa_B a\sigma_+^{(B)} + h.c.) \\ &+ \frac{\hbar C_3}{R^3}(\sigma_+^{(A)}\sigma_-^{(B)} + \sigma_-^{(A)}\sigma_+^{(B)}) \end{aligned} \qquad (2)$$

Here ω_c is the frequency of the cavity-mode, $\omega_A \simeq \omega_B$ are the atomic transition frequencies, and $\kappa_{A,B}$ are the coupling parameters of the atom A(B) to the cavity mode; C_3 is the dipole-dipole coupling coefficient, $\sigma_\pm$ and σ_z are the atomic pseudo-spin operators and $a(a^\dagger)$ is annihilation(creation) operator of the field mode.

The adiabatic Hamiltonian in Eq.(2) is exactly solvable [4] in the basis of three coupled atom-field states $\mid e_A, g_B, 0 >$, $\mid e_B, g_A, 0 >$ and $\mid g_A, g_B, 1 >$ where $e_j(g_j)$ represents the excited (ground) state of the jth atom (j=A,B) while 0 and 1 are the number of photons in the cavity mode. We can write $H_{ad}\chi_i = \hbar\omega_i\chi_i$ $(i = 1, 2, 3)$, with $\omega_1 < \omega_2 < \omega_3$. As discussed in Ref. [4], for $R \to 0$, $\omega_3 \to \omega_s = \omega_A + C_3/R^3$, $\omega_2 \to \omega_c$, and $\omega_1 \to \omega_a = \omega_A - C_3/R^3$. This means that the near-resonant cavity mode is then decoupled from the symmetric and antisymmetric states $\mid s, a\rangle = 2^{-1/2}(\mid e_A, g_B, 0 > \pm \mid e_B, g_A, 0 >)$. The symmetric-state and cavity-mode contributions become increasingly hybridized as R increases [4]: $\omega_1 \simeq \omega_a$, $\omega_2 \simeq \frac{1}{2}(\omega_s + \omega_c - \Omega)$, $\omega_3 \simeq \frac{1}{2}(\omega_s + \omega_c + \Omega)$; with $\Omega = \sqrt{2(\kappa_A + \kappa_B)^2 + (\omega_s - \omega_c)^2}$. The potentials ω_1 and ω_2 exhibit a pseudo-crossing at a relatively large interatomic separation ($\sim 1000a_0$, where a_0 is the Bohr radius) depending on the coupling strength of the atoms with the cavity field. The potential ω_2 has a minimum at the pseudo-crossing point (R_c), and so it can behave as a potential well supporting quasi-bound states. We illustrate these long-range adiabatic potentials in Fig.1 for a pair of Cs atoms with levels $6S_{1/2}$ and $6P_{3/2}$ ($\omega_A = \omega_B = 3.5172 \times 10^{14} Sec^{-1}$), with atom-cavity parameters as in the experiment of Ref. [7] and realistic dipole-dipole [8] coupling parameter. The larger the atom-field coupling strength, the deeper is the potential well (ω_2) with the minimum point R_c shifted towards shorter separations(Inset(a) to Fig.1). For the cavity parameters of Ref. [7], the depth of the binding potential should lie in the radio-frequency regime. An increase of the atom-cavity coupling strength by 2 orders of magnitude will enable the binding potential ω_2 to support

bound states separated by microwave frequencies. Inset(b) to Fig.1 shows the effect of cavity-atom detuning on the value of the potential ω_2 at R_c. For both red and blue detunings ω_2 acts as a binding potential, but increasing red detuning leads to more attractive ω_2 and reduced R_c, while the opposite is true for blue detuning.

The potentials drawn in Fig.1 must be correlated to the short-range potentials [8] in which the interatomic repulsion due to the overlap of electron charge distributions is much larger than the atom-cavity coupling. For the Cs($6P_{3/2}$)-Cs($6P_{1/2}$) system, the short-range limit ($R \leq 28a_0$) of potential ω_1 should be correlated to the A $^1\Sigma_u^+$ potential, which at long ranges corresponds to the $S - P_{3/2}$ asymptote [8]. We interpolate the curve ω_1 so that it can merge with the model A $^1\Sigma_u^+$ potential at separations comparable to the equlibrium position at $R \simeq 10a_0$. Since the field-atom coupling strength $\kappa_{A(B)}$ varies sinusoidally along the standing-wave cavity mode, a pair of ultracold atoms is more likely to become quasi-bound by the binding potential ω_2 in the vicinity of an antinode than elsewhere. As we show in Fig.1, the internuclear separation R for this quasi-bound state and a cavity mode of wavelength λ_c typically satisfies the criterion $R << \lambda_c$ (the pseudocrossing separation $R_c \simeq 10\%$ of λ_c for Cs-Cs). Thus a high-Q cavity loaded with ultracold atoms may give rise to periodic distribution of giant quasibound diatoms near the cavity mode antinodes. Within the range of separations R for which the adiabatic potential is significant, the atom-field coupling parameters κ_A and κ_B remain nearly constant.

In order to elucidate the formation of quasibound states of two atoms by cold atomic photoassociation [9] or diatomic photodissociation inside a high-Q cavity, we adopt multi-channel scattering theory [10]. Let the eigenfunction of the Hamiltonian $H = H_k + H_{ad}$ with angular momentum l be given by $\psi_l = \Sigma_{i=1}^3 (\phi_i \chi_i)_l$. From the Schroedinger equation $H\psi_l = E\psi_l$, we obtain, after some algebra,

$$\frac{d^2\Phi}{dR^2} + 2\tau^{(1)}\frac{d\Phi}{dR} = \frac{2\mu}{\hbar^2}(U + \frac{l(l+1)}{R^2} - E)\Phi \qquad (3)$$

where $\Phi = (\phi_1\ \phi_2\ \phi_3)^T$ is the solution vector and $U = \hbar$ diag.$(\omega_1, \omega_2, \omega_3)$ is the diagonal eigenvalue matrix, the nonadiabatic-coupling matrix $\tau^{(1)}$ has the elements $\tau_{ij}^{(1)} = \langle \chi_i \mid \frac{d}{dR} \mid \chi_j \rangle = -\tau_{ji}^{(1)}$ $(i, j = 1, 2, 3)$, and the higher order terms $\tau_{ij}^{(2)} = \langle \chi_i \mid \frac{d^2}{dR^2} \mid \chi_j \rangle$ have been dropped, consistently with the low-energy regime. For the sake of convenience, Eq.(3) can be transformed into the following form [10]

$$(\frac{d^2}{dR^2} + P^2 - W - \frac{l(l+1)}{R^2})\tilde{\Phi} = 0 \qquad (4)$$

where $\tilde{\Phi} = T\Phi$, and $W = \frac{2\mu}{\hbar^2}[TUT^{-1} - \hbar$ diag.$\{\omega_1(R \to \infty), \omega_2(R \to \infty), \omega_3(R \to \infty)\}]$; T is a transformation matrix $T = exp(-\int_{R_\infty}^{R} \tau^{(1)} dR)$, with the lower limit of the integration at an arbitrary large separation denoted by R_∞ where all the potentials are flat; P is a 3×3 diagonal matrix whose diagonal elements are the $P_i = \hbar^{-1}\sqrt{2\mu\{E - \hbar\omega_i(R \to \infty)\}}$, $i = 1, 2, 3$.

Equation(4) represents a compact form of the scattering equations of three coupled channels, which are to be solved under the following boundary conditions: $\tilde{\phi}_{ml}^{(i)}(R \to 0) \sim 0$ and $\tilde{\phi}_{ml}^{(i)}(R \to \infty) \sim P_m^{-1} Sin(P_i R - \frac{l\pi}{2})\delta_{mi} + P_i P_m^{-1} Cos(P_m R - \frac{l\pi}{2}) K_{mi}^l$, where the reaction matrix K is related to the S-matrix (see below) by $K^l = i(1 - S^{(l)})(1 + S^{(l)})^{-1}$. Here i labels the incident channel, along with the angular momentum l. From now on we focus on s-wave ($l = 0$) scattering, which is appreciable for ultra-cold atoms [11], and omit the label l. The regular wavefunction which is a solution of the multichannel scattering equations can then be expressed in matrix form [10] as

$$\tilde{\tilde{\Phi}}(R) = J + \int_0^R dR' G(R, R') W(R') \tilde{\tilde{\Phi}}(R') \qquad (5)$$

where $\tilde{\tilde{\Phi}}$ is a 3×3 matrix with its ith column being the regular part of the solution vector $\tilde{\Phi}$ for the ith incident channel, J and G are 3×3 diagonal matrices with the nth diagonal element being $J_n = Sin(P_n R)/P_n$ and

$$\begin{aligned} G_n = & P_n^{-1} Sin(P_n R) Cos(P_n R') \\ & - P_n^{-1} Cos(P_n R) Sin(P_n R') \end{aligned} \qquad (6)$$

These solutions must be supplemented by the analysis of the poles of the S-matrix

$$S = P^{\frac{1}{2}} F(-P) F^{-1}(P) P^{-\frac{1}{2}} \qquad (7)$$

which is expressed in terms of the Jost function [10]

$$F(P) = 1 + \int_0^\infty dR exp(iPR) W \tilde{\tilde{\Phi}} \qquad (8)$$

In the absence of cavity dissipation, the bound states are given by the real poles of the S matrix whose energy E is below the lowest threshold, i.e., below $\hbar\omega_1(R \to \infty)$, so that all the corresponding channel momenta $\hbar P_i (i = 1, 2, 3)$ have positive imaginary values. The scattering resonances are given by the complex poles of the S matrix, with energies E above the lowest threshold, the imaginary part of the complex energy being negative. Resonances should be observed as a signature of the cavity-confined quasi-bound states. In Fig.2 we show the variation of scattering cross-section (σ_{11}) against energy with only one (lowest) open channel, the remaining channels being closed. This variation reveals the cavity-induced resonances. They have an effective width $\Gamma_{eff} = \Gamma_R + \Gamma_c$, where Γ_R is the resonance width in an ideal (lossless) cavity and Γ_c is the rate of cavity dissipation (cavity linewidth). For the case of Fig.1 our estimate yields $\Gamma_R \sim 2$ MHz. If we take [7] $\kappa_A \simeq 120$ MHz and $\Gamma_c \sim 40$ MHz, the resonances associated with individual vibrational states of ω_2 cannot be resolved. However, for

cold Rydberg atoms [12] in a high-Q microwave cavity [13], these resonances are shown to be resolvable due to the much larger ratio of κ_A/Γ_c.

One may observe the predicted resonances, e.g., by populating loosely bound states of the Cs_2 potential A $^1\Sigma_u^+$ [8] that are below the dissociation threshold by an amount ranging from 0 to 100 MHz, via photoexcitation of the ground molecular potential X $^1\Sigma_g^+$. Nonadiabatic effects at separations of a few nm will then produce a mixure of $^1\Sigma_u^+$ and $^3\Pi_u$ states [14]. The alternative is photoassociation [9]: As the two ground-state (S-state) cold atoms approach each other inside the cavity, they should be excited by a single photon. By tuning the frequency of this photon, the two atoms can be raised to the desired adiabatic potential ω_1 or ω_2, their relative velocity can be controlled and determine the scattering-channel inputs in Eq.(5).

In order to evaluate the characteristics of resonance fluorescence associated with the discussed effect, we have approximated the potential ω_2 given in Fig.1 by the Morse model, for which we can determine the vibrational states supported by that potential. The vibrational frequency ω_{2v} in the quasibinding potential ω_2 depends on the orientation of the molecular axis relative to the cavity axis, since the adiabatic Hamiltonian given in Eq.(2) is a function of the angle between the atomic dipole and the cavity field (via $\kappa_{A,B}$). By applying the Landau-Zenner-Stueckelberg (LZS) [10] semiclassical treatment of nonadiabatic coupling near the pseudocrossing of ω_1 and ω_2, we have calculated the energy-shifts of each of those vibrational states. The Franck-Condon spectrum of fluorescence for the transition from vth level of ω_2 to the ground state (gg) of the diatom has been calculated for an exciting photon polarized along the X-axis, and an emitted photon along the Z axis, which is the direction of the cavity field. It can then be expressed as

$$I_{2v\to gg}(\omega) = C\int_\theta d\theta Sin(\theta) W_\theta \{\frac{\Gamma_{eff}^2}{(\omega-\omega_{2v}(\theta))^2+\Gamma_{eff}^2}\} \times \mid \int dR < \phi_{2v}\chi_2 \mid a(\sigma_+^{(A)}+\sigma_+^{(B)}) \mid \phi_{gg} > \mid g_A, g_B, 1 >\mid^2 \quad (9)$$

Here C is a constant, Γ_{eff} is the effective linewidth as before, $\omega_{2v}(\theta)$ is corrected for LZS pseudocrossing effects and W_θ is a weight factor, both depending on the random angle (θ) between the Z-axis and the molecular axis: $W_\theta = Sin^2(\theta)$ and $W_\theta = Cos^2(\theta)$ [14] for the Σ and Π symmetry, respectively. The wavefunctions ϕ_{2v} and ϕ_{gg} represent the vth vibrational state in the ω_2 potential and the radial ground state, respectively. For a ϕ_{2v} state with Σ symmetry, the dipole selection rule forces ϕ_{gg} to have the angular momentum $l=1$ in the S-S asymptotic ground state potential ($-1/R^6$). We have $\phi_{gg} \simeq R j_1(\sqrt{2\mu E_{gg}}R/\hbar)$ [11], where j_1 is the $l=1$ spherical Bessel function and E_{gg} is the ground-state (S-S) energy, which is assumed to be of the order of one-photon recoil energy for the transition $P_{3/2}\to S_{1/2}$. We display the spectrum [Eq.(9)] in Fig.3.

Spectral peaks in the range of the potential depth ω_2 are indications of the cavity-confined quasi-bound diatomic states. Our estimates show that for the parameters of Fig.1 and Ref. [7], the vibrational-line spacing is well below the cavity linewidth ($\Gamma_c \sim 40MHz$). In order to resolve these lines properly, the κ_A/Γ_c ratio should be further increased, e.g., by using cold Rydberg atoms in a high-Q cavity [12,13] (see Fig.2b). Yet, even in the absence of optimal resolution, the spectral signature of the quasibinding effect in Fig.3 is unambiguous, especially for the Π symmetry.

To conclude, we have demonstrated several unusual dynamical features obtainable in the strong-coupling cavity regime of diatomic collisions or dissociation. These features are associated with vibrational quasibound states, which can be excited by intracavity photoassociation of colliding cold atoms via single photon absorption at a frequency below the normal dissociation threshold. An alternative is intracavity excitation of a cold dimer by single-photon absorption at a frequency just below the dissociation threshold. The prediction of cavity-induced giant quasi-bound cold diatomic complexes is the first indication that modifications of molecular collision dynamics by cavity QED may be used to 'engineer' novel metastable states of matter, which will live as long as the cavity holds the photon inside.

This work has been supported by ISF, EU(TMR) and Minerva grants. We thank Dr. B. Galanti for his help with numerical computations.

[1] B.G. Englert, J. Schwinger, A.O. Barut, and M.O. Scully, Europhysics Lett. **14**, 25 (1991); M.O. Scully, G.M. Meyer, and H. Walther Phys.Rev.Lett. **76**, 4144 (1996); G.M. Meyer, M.O. Scully, and H. Walther, Phys.Rev.A **56**, 4142 (1997); M. Loffler, G.M. Meyer, M. Schroeder, M.O. Scully, and H. Walther, Phys.Rev. A **56**, 4153 (1997); M. Schroeder, K. Vogel, W.P. Schleich, M.O. Scully, and H. Walther, Phys.Rev.A **56**, 4164 (1997).

[2] Y. Japha, V.M. Akulin, and G. Kurizki, Phys.Rev.Lett. **80**, 3739 (1998); Y. Japha, and G. Kurizki, Phys.Rev.Lett. **77**, 2909 (1996).

[3] S. Inouye, M.R. Andrews, J. Stenger, H.-J. Miesner, D.M. Stamper-Kurn, and W. Ketterle, Nature **392**, 151 (1998); Ph. Courteille, R.S. Freeland, and D.J. Heinzen, F.A. van Abeelen, and B.J. Verhaar, Phys.Rev.Lett. **81**, 69 (1998); H.M.J.M. Boesten et al., Phys.Rev.Lett. **77**, 5194 (1996).

[4] G. Kurizki, A.G. Kofman, and V. Yudson, Phys.Rev. A **53**, R35 (1996).

[5] E. V. Goldstein and P. Meystre, Phys.Rev. A **56**, 5146(1997).

[6] G.M. Meyer, and G. Yeoman, Phys.Rev.Lett. **79**, 2650 (1997); P. Kochan et al., Phys.Rev.Lett. **75**, 45 (1995).
[7] C.J. Wood, M.S. Chapman, T.W. Lynn, and H.J. Kimble, Phys.Rev.Lett. **80**, 4157 (1998); G. Rempe, Appl.Phys.B **60**, 233 (1995).
[8] M. Marinescu and A. Dalgarno, Phys.Rev.A **52**, 311 (1995); Y.B. Band and P.S. Julienne, Phys.Rev. A **46**, 330 (1992).
[9] P.D. Lett, P.S. Julienne, W.D. Phillips, Annu.Rev. Phys.Chem. **46**, 423 (1995).
[10] R.G. Newton, *Scattering Theory of Waves and Particles* (McGraw Hill, 1966); J.R. Taylor, *Scattering Theory* (Wiley, 1972); M.S. Child, *Molecular Collision Theory* (Academic, 1974); M. Baer, in *Molecular Collision Dynamics*, editor J.M. Bowman, (Springer, 1983).
[11] J. Weiner, Adv.At.Mol.Opt.Phys. **35**, 45 (1995); P. Pilet et al., J.Phys.B **30** 2801 (1997).
[12] I. Mourachko, D. Comparat, F. de Tomasi, A. Fioretti, V.M. Akulin, and P. Pillet, Phys.Rev.Lett. **80**, 253 (1998).
[13] M. Brune et al., Phys.Rev.Lett. **77**, 4887 (1996); H. Walther, Phys.Scripta T**76**, 138 (1998).
[14] G. Kurizki, Phys.Rev. A **43**, R2599 (1991); G. Kurizki and A. Ben-Reuven, Phys.Rev.A **32**, 2560 (1985).

FIG.1 Adiabatic potentials (in MHz) as a function of interatomic separation (in Bohr radii a_0) for Cs atoms, $\omega_c - \omega_A = 1.0MHz$, $\kappa_A = 120MHz$, at short separations and near the pseudocrossing (equilibrium) position $R_c \sim 2000a_0$, $\kappa_B = 0.8\kappa_A$. Inset(a): Depth of ω_2 (in MHz) and position R_c (in Bohr radius) as a function of atom-field coupling strength κ_A (in MHz). Inset(b): Minimum of ω_2 (in MHz) at R_c as a function of cavity-atom detuning (in MHz) for red ($\omega_c < \omega_A$) and blue ($\omega_c > \omega_A$) detuning.

FIG.2 (a) S-wave scattering cross section σ_{11} (in cm^2) as a function of energy in MHz or momentum $\hbar P_1$ (in 10^{-22} gm cm/sec) for two Cs-atoms sharing an optical excitation in a cavity without losses ($\Gamma_c = 0, \Gamma_R = 2$ MHz) and with loss ($\Gamma_c = 5$ MHz, dashed) with parameters as in Fig.1. (b) Idem, for Rydberg Cs-atoms sharing an excitation near $\omega_A = 600GHz$, $\kappa_A = 150KHz$, $\kappa_B = 0.99\kappa_A$, and $\omega_c - \omega_A = 1.0KHz$ for an ideal cavity (solid line) and dissipative cavity with $\Gamma_c = 2KHz$ (dashed lines).

FIG.3 Spectrum (arbitrary scale) of $\mid \chi_2\phi_{2v}\rangle \rightarrow \mid g_Ag_B, 1\rangle$ transition for Σ and Π symmetry of the quasi-binding state with $\Gamma_{eff} = 8MHz$ and randomly oriented diatomic axis. The parameters are as in Fig.1.

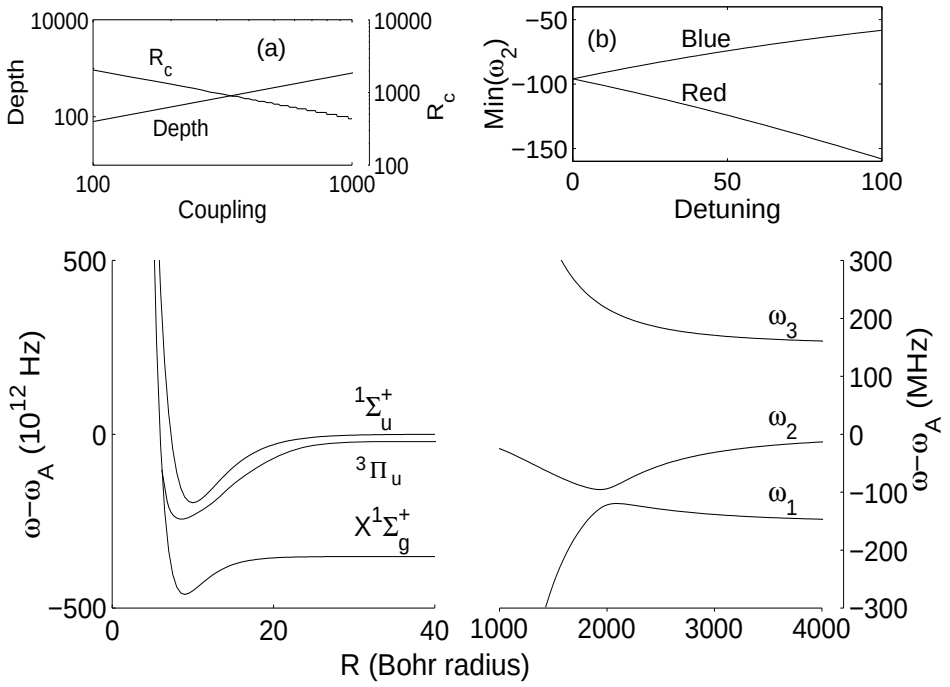
10000
100
Depth
100
1000
Coupling
(a)
R_c
Depth
10000
1000
100
R_c
−50
−100
−150
Min(ω_2)
(b)
Blue
Red
0
50
100
Detuning
500
0
−500
ω−ω_A (10^12 Hz)
0
20
40
R (Bohr radius)
1Σ+u
3Πu
X1Σ+g
ω3
ω2
ω1
1000
2000
3000
4000
300
200
100
0
−100
−200
−300
ω−ω_A (MHz)

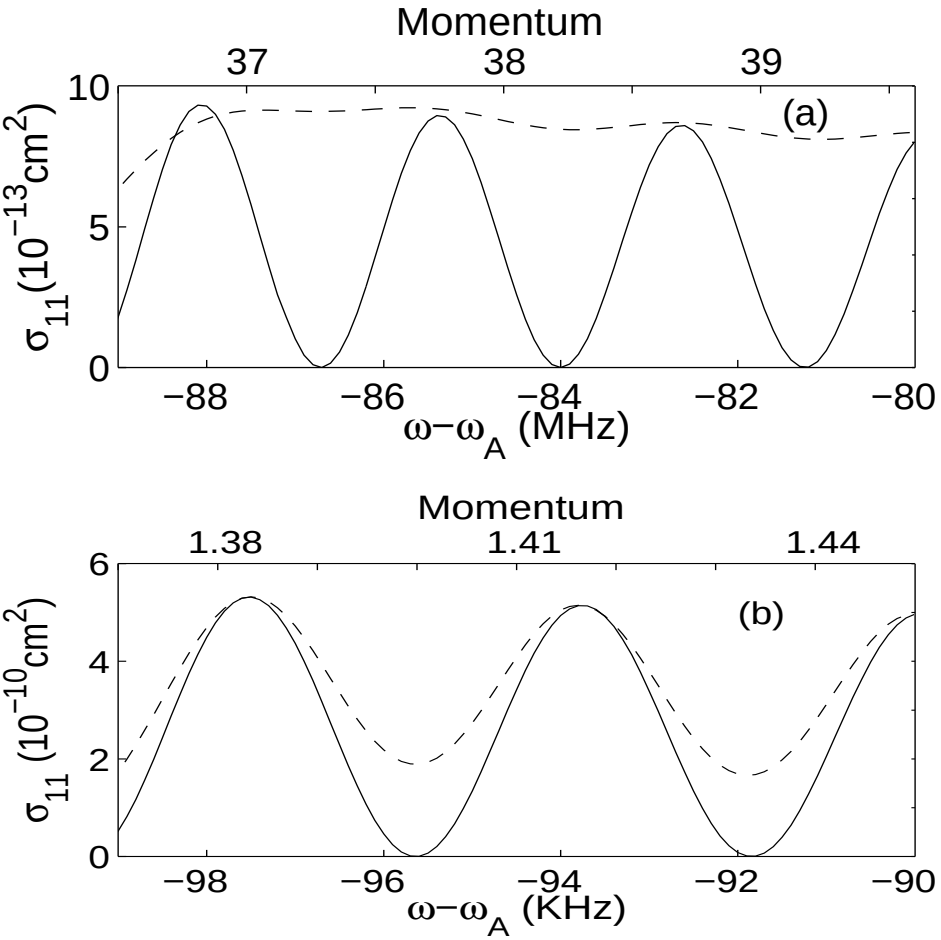
Momentum
37
38
39
10
5
0
(a)
$\sigma_{11}(10^{-13}cm^2)$
−88
−86
−84
−82
−80
$\omega-\omega_A$ (MHz)
Momentum
1.38
1.41
1.44
6
4
2
0
(b)
$\sigma_{11}(10^{-10}cm^2)$
−98
−96
−94
−92
−90
$\omega-\omega_A$ (KHz)

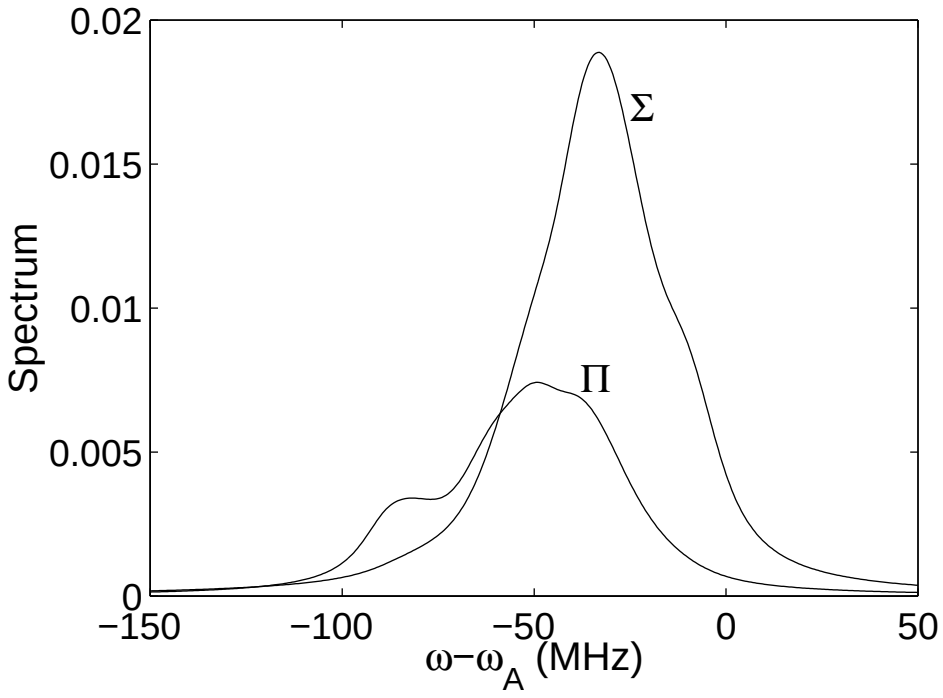
0.02
0.015
0.01
0.005
0
Spectrum
Σ
Π
−150
−100
−50
0
50
ω−ω_A (MHz)